

# Calculation of optical modes in large emission area photonic crystal surface-emitting lasers

Mindaugas Radziunas\*, Eduard Kuhn\*, Hans Wenzel†, Ben King†, and Paul Crump†

\*Weierstrass Institute (WIAS), Mohrenstrasse 39, 10117 Berlin, Germany. Email: Mindaugas.Radziunas@wias-berlin.de

†Ferdinand-Braun-Institut (FBH), Gustav-Kirchhoff-Str. 4, 12489 Berlin, Germany.

**Abstract**—We discuss numerical challenges in constructing and resolving spectral problems for photonic crystal surface-emitting lasers with large (up to several  $\text{mm}^2$ ) emission area. We show that finite difference schemes with moderate and large domain discretization steps provide sufficient accuracy of several major (lowest-threshold) modes of particular device designs.

Semiconductor diode lasers are small, efficient, and relatively cheap devices used in many modern applications. Multiple applications require emission powers exceeding several ten watts from a single diode and up to a few kilowatts from a combined laser system. In this work, we consider photonic crystal (PC) surface-emitting lasers (SELs), see Fig. 1, which, in contrast to edge-emitting broad-area lasers, are capable of emitting high-power (up to 80 W pulsed [1] and 50 W CW [2]) beams of nearly perfect quality in the ( $z$ ) direction, perpendicular to the ( $x/y$ ) plain of the active material. The critical part of PCSELs, enabling an efficient coupling of optical fields generated within the active layer and their redirection along the  $z$  axis, is a 2-dimensional PC layer. In simple cases, it can be vertically homogeneous or consist of several vertically homogeneous layers (e.g., three layers as shown in Fig. 1).

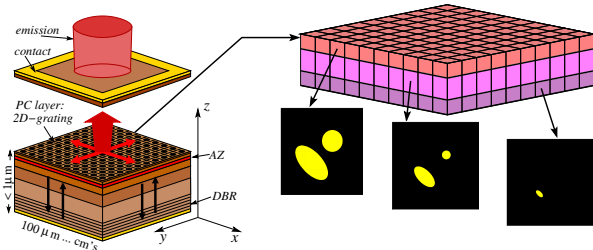


Fig. 1. Schematic depiction of exemplary PCSEL with the PC layer consisting of three vertically homogeneous sublayers.

The periodic features of the PC layer in best PCSEL devices are filled with air, which guarantees a large refractive index contrast and, thus, a large coupling of counter- and cross-propagating fields within the PC. This high index contrast allows for the formation of firmly centered main modes already in moderate ( $\sim 0.1 \text{ mm}^2$ ) emission area PCSELs. Formation of similarly centered modes in PCSELs having PC layers with less contrast in refractive indices will require larger emission areas and, thus, more efficient numerical algorithms to cope with the increased size.

To model high-power  $\gg 0.1 \text{ mm}^2$  PCSELs, we exploit a three-dimensional coupled-wave model [3], [4] derived for TE mode operation, relying on the dielectric function's periodicity

within the PC layer and corresponding Fourier expansion of this function and the electrical fields. Due to a special choice of the lattice parameter  $a$ , four nonvanishing basic waves (space and time-dependent field expansion components at  $e^{-i\beta_0(mx+ny)}$ ,  $\beta_0 = \frac{2\pi}{a}$ ,  $|m| + |n| = 1$ ) can be written as  $u^\pm(x, y, t)\Theta_0(z)$  and  $v^\pm(x, y, t)\Theta_0(z)$ . The fundamental guided mode  $\Theta_0(z)$  and related propagation factor  $\beta \approx \beta_0$  solve a one-dimensional Helmholtz problem. Dynamic equations [3] for slowly varying field amplitudes  $u(x, y, t) = (u^+)$ ,  $v(x, y, t) = (v^+)$  can be written as

$$\begin{aligned} \frac{1}{v_g} \frac{\partial}{\partial t} \begin{pmatrix} u \\ v \end{pmatrix} &= \mathcal{H}(\Delta\beta(N)) \begin{pmatrix} u \\ v \end{pmatrix} + F_{sp}, \quad (x, y) \in [0, L] \times [0, L], \\ \text{B.C.:} \quad u^+|_{x=0} &= u^-|_{x=L} = v^+|_{y=0} = v^-|_{y=L} = 0, \\ \mathcal{H}(\Delta\beta(N)) &= i\mathbf{C} - \begin{pmatrix} \sigma \frac{\partial}{\partial x} & \mathbf{0} \\ \mathbf{0} & \sigma \frac{\partial}{\partial y} \end{pmatrix} - i\Delta\beta(N), \quad \sigma = \begin{pmatrix} 1 & 0 \\ 0 & -1 \end{pmatrix}. \end{aligned}$$

Here  $v_g$ ,  $F_{sp}$ , and  $\Delta\beta(N)$  are the group velocity, the Langevin noise sources, and the relative propagation factor, which depends on the local carrier density governed by the additional diffusive carrier rate equation. For any fixed  $N(x, y)$ ,  $\Delta\beta(N) = \overline{\Delta\beta}$  is a function of ( $x, y$ ). The field equations above are linear w.r.t.  $(u)$  and imply the spectral problem [4],

$$\mathcal{H}(\overline{\Delta\beta})\Theta = \Lambda\Theta, \quad \Theta(x, y) = \begin{pmatrix} \Theta_u \\ \Theta_v \end{pmatrix} \text{ satisfies B.C..} \quad (1)$$

This problem, given by a system of four 2-D PDEs, is very important when designing PCSEL devices. For example, the location of several major (low-threshold) modes in the case of vanishing or spatially uniform  $\overline{\Delta\beta}$  ("cold cavity" PCSEL case) allows a prediction of lasing threshold and an estimation of the side mode damping in the close-to-threshold state.

To complete the definition of the spectral problem, one has to construct a complex  $4 \times 4$  field coupling matrix  $\mathbf{C}$  entering operator  $\mathcal{H}$ . Estimation of  $\mathbf{C}$  is a nontrivial task: it requires knowledge of  $\Theta_0(z)$ , Fourier expansion coefficients of the dielectric function  $\xi_{m,n}$ , and Green's functions  $G_{n,m}(z, z')$  solving the inhomogeneous Helmholtz problem

$$\left[ \frac{d^2}{dz^2} + k_0^2 n_0^2(z) - (m^2 + n^2)\beta_0^2 \right] G_{m,n}(z, z') = -\delta(z - z')$$

along the vertical axis. Typically [3], [4],  $\mathbf{C}$  is represented as a sum of a nonhermitian matrix  $C_{rad}$  (out-of-plane coupling via radiative waves with  $m = n = 0$ ), and two Hermitian matrices  $C_{1D}$  (1D coupling of counterpropagating waves) and  $C_{2D}$  (2D coupling via higher order,  $|m| + |n| > 1$ , modes). The last matrix is an infinite sum,  $C_{2D} = \sum_{m,n} C_{2D}^{(m,n)}$ . In our

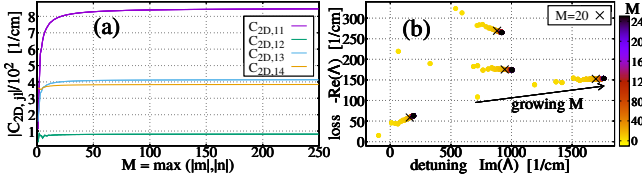


Fig. 2. Construction of matrix  $\mathbf{C}$  for a double-lattice air-hole PCSEL similar to that of Ref. [3]. (a): convergence of elements of  $\mathbf{C}_{2D}$  and (b): corresponding eigenvalues of  $\mathbf{C}$  with increasing number  $M$  of Fourier modes.

calculations, we truncate this sum, accounting only for  $\mathbf{C}_{2D}^{(m,n)}$  with  $\{|m|, |n|\} \leq M$ . In Fig. 2, we analyze the precision of our calculations as a function of  $M$ . Panel (a) shows the amplitudes of four elements of this matrix as functions of  $M$ . We achieve 1% relative error of these elements at  $M \approx 90$ . Panel (b) reveals changes in the spectra of  $\mathbf{C}$ , depending on the truncation factor  $M$  (yellow: small  $M$ , dark: large  $M$ ). Already for  $M = 20$  (black crosses, left from the accumulation of dark bullets), the spectra can be resolved satisfactorily.

The matrix components  $\mathbf{C}_{2D}^{(m,n)}$  depend on the fundamental mode intensity and Fourier coefficients  $\xi_{m\pm 1, n}$ ,  $\xi_{m, n\pm 1}$  within each PC layer and double integrals  $\int_{S_k} \Theta_0^*(z) \int_{S_l} G_{m,n}(z, z') \Theta_0(z') dz' dz$  for each combination of PC layers  $S_k$  and  $S_l$ . Calculating these double integrals using standard domain discretization-based numerical approximations for multiple combinations of  $(m, n)$  and, possibly, multiple PC sublayers is a hard numerical task that can take hours or even days. Fortunately,  $\Theta_0$  and  $G_{m,n}$  can be written using transfer matrices and exponential functions, such that the required integral relations can be expressed by analytic formulas. An advantage of our approach is a significant speedup in calculations and increased precision of matrix estimation (large  $M$  can be used, discretization-induced errors are absent). In this way, we could estimate  $\mathbf{C}$  using  $M = 500$  for PCSELS with 1 and 3 PC layers in 25 and 108 seconds, whereas similar work for a PCSEL with 6 PC and 27 overall layers using  $M = 20$  took 12 seconds. Notably, analytic formulas representing  $G_{m,n}$  and related double integrals for large  $|m|$  and  $|n|$  should be used with care since we handle very large and small exponentials  $\sim e^{\pm\sqrt{m^2+n^2}\beta_0 z}$ . Our first simulations using built-in sinh and cosh functions within transfer matrices failed at  $M = 25$ . By treating large exponentials within these functions separately, we could run calculations up to  $M \approx 200$ . After additionally accounting for computer-arithmetic problems (such as  $\varepsilon + 1 - 1 \equiv 0$  whereas  $\varepsilon + (1 - 1) \equiv \varepsilon$  for  $|\varepsilon| < 10^{-16}$ ), calculations can be done now for  $M = 500$  and more.

Let us return to the solution of the spectral problem (1). Since we cannot resolve this problem analytically, we rely on fully numerical procedures. The algorithm is based on field discretization using a uniform staggered spatial mesh,  $\Theta(x, y) \mapsto \Theta_h$ , and approximation of the functions and their spatial derivatives with central difference schemes. As a result, Eq. (1) is approximated by the generalized spectral problem

$$A_h \Theta_h = P_h \Lambda_h \Theta_h. \quad (2)$$

$A_h, P_h$  are non-hermitian complex sparse  $4n \times 4n$  matrices,  $n$  is the number of the mesh steps along each side of the calculation domain. This (finite-dimensional) numerical scheme does not provide all (i.e., an infinite number of) modes of the original problem; the numerically induced error in the approximation of the resolved modes grows with increasing mesh step  $h = \frac{L}{n}$ . For large-area PCSELS suitable for very high powers (e.g.,  $L = 4$  mm) and moderate discretization steps (e.g.,  $h = 10 \mu\text{m}$ ,  $n = 400$ ), Eq. (2) defines nearly a million modes, which can not all be found due to computer memory and time constraints. Fortunately, only a few modes are important, such that we can exploit the sparseness of the matrices and look only for several dominant modes preselected in preliminary calculations with a rough numerical mesh, see the light blue dots and the five main modes indicated with symbols in Fig. 3(a). Already the initial calculations provide sufficiently good precision of the dominant modes; see panels (b) and (c) showing a convergence of three main modes with an increase of  $n$  from 8 to 28.

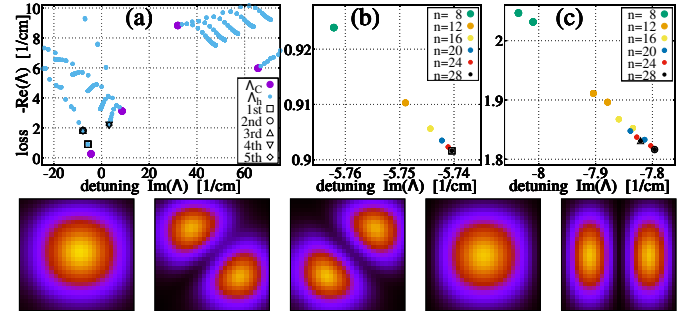


Fig. 3. (a): main eigenvalues of Eq. (2) for  $n = 28$  (light blue) and of  $\mathbf{C}$  (magenta). (b),(c): convergence of the main (b) and the 2nd/3rd (c) eigenvalues with growing number of mesh steps. Bottom row: total field intensity of five dominant modes, indicated with symbols in upper panels.  $L = 4$  mm, other parameters are as in Fig. 2, only the refractive index contrast in the PC is reduced.

In conclusion, we demonstrated how rough numerical meshes with  $n \sim 20$ , 2nd-order precision finite difference schemes, and standard spectral solvers provide a good approximation of a few major optical modes. Once better precision or more modes are required, we exploit higher-order numerical schemes, which reduce discretization-induced errors by a few orders or more, depending on the mesh factor  $n$ .

This work was performed in the frame of the project ‘‘PCSELence’’ (K487/2022) funded by the German Leibniz Association.

## REFERENCES

- [1] Inoue et al., ‘‘Self-evolving photonic crystals for ultrafast photonics,’’ *Nat. Commun.*, **14**, 50, 2023.
- [2] Yoshida et al., ‘‘50W continuous-wave operation of a 3mm-diameter photonic-crystal surface-emitting laser,’’ *CLEO, SFIQ.5*, May 12, 2023.
- [3] Inoue et al., ‘‘Comprehensive analysis of photonic-crystal surface-emitting lasers via time-dependent three-dimensional coupled-wave theory,’’ *Phys. Rev. B*, **99**, 035308, 2019.
- [4] Y. Liang et al., ‘‘Three-dimensional coupled-wave analysis for square-lattice photonic crystal surface emitting lasers with transverse-electric polarization: finite-size effects,’’ *Optics Express*, **20**, 15945, 2012.